Response to reviewer

We gratefully thank the reviewer for the constructive comments and suggestions to improve the manuscript. Below are the detailed point-to-point responses to the reviewer's comments. For clarity, the reviewer's comments are listed below in *black italics*, while our responses and changes in the manuscript are shown in blue and red, respectively. The changes in the revised manuscript and supporting materials are also highlighted.

Anonymous Referee #1 (RC1)

This paper describes measurements of rainwater samples collected on Mount Tai in eastern China. INP concentrations with and without heat treatment were measured alongside ions in rainwater. INP concentrations in air were estimated based on an assumed cloud water content. Variation of INP concentrations is briefly examined across the seasons measured. An attempt is made to use PMF analysis to describe the aerosol populations associated with INP concentrations, though this piece of the work is critically flawed in my opinion, described in more detail below. Due to the lack of formal error analysis of the INP data and the flaws with the PMF analysis and interpretation, I do not believe this manuscript is publishable in it's current form. More rigorous analysis could be done with the dataset described and a heavily changed version could be considered for a future submission.

Response: We thank the reviewer for the critical comments and valuable suggestions, which are very helpful for improving our study. The reviewer's main concerns related to (1) the lack of formal error analysis of the INP data and (2) the flaws with the PMF analysis. Below we first address these major concerns, and then provide detailed point-to-point replies to the specific comments.

(1) We fully agree with the reviewer on the necessity of including the error analysis. In the INP measurements, the stochasticity of nucleation is the primary source of uncertainty. In the revised manuscript, we used the method proposed by Barker (2002) and O'sullivan et al. (2018) to calculate the confidence intervals.

$$\mu(T) + \frac{\left(Z_{\alpha/2}\right)^2}{2n} \pm Z_{\alpha/2}\left[4\mu + \frac{\left(Z_{\alpha/2}\right)^2}{n}\right]^{0.5} /4n^{0.5}$$

where μ(T) is the number of INPs per droplet, n is the droplet number (90 in our experiments), Zα/2 is the standard score at a confidence level α/2 (1.96 for a 95% confidence interval).

In addition to nucleation stochasticity, other potential sources of uncertainty have been suggested, including aerosol collection and nucleus multiplication. However, these do not introduce a large bias in derived INP concentrations, as noted by Vali (1974) and Wright et al. (2014). Furthermore, the influence of dissolved solutes and chemical aging on INP concentrations in rainwater are estimated to be less than an order of magnitude at certain

temperatures (Petters and Wright, 2015). Based on these considerations, we did not apply further corrections in this study.

(2) To assess the robustness of our PMF results, we removed the winter samples and re-conducted the PMF analysis twice, using the dataset with and without the N_{INP_air} parameter. The two source profiles are essentially identical, and each factor clearly identified. This indicates that the inclusion of N_{INP_air} has minimal influence on factor classification.

Moreover, in the PMF analysis including N_{INP_air}, 95% of the residuals for all parameters fell within the range of -3 to +3. Specifically, the residuals of N_{INP_air} ranged from -2.3 to +2.7, which lies well within the acceptable range of -3 to 3 suggested by Zhang et al. (2024b). These results support the conclusion that the interpretation of INP data within the PMF framework is robust and meaningful.

Further details are provided in the following point-by-point responses.

Major comments:

Section 2.2 – There is no discussion of error analysis. There will be large errors associated with counting uncertainties in the INP measurements and the assumption of cloud water content. Additionally, field blanks should have been performed in order to assess the cleanliness of handling procedures of the rainwater samples. If dilutions were performed additional analysis of dilution water must be performed. INP concentrations would then need to be corrected for background INPs in field blanks and dilution water (if used), with uncertainties propagated. My understanding is that incorporating these uncertainties into the PMF analysis could drastically change the results of the manuscript.

Response: We fully agree with the necessity of the error analysis in this study. The stochasticity of nucleation is the primary source of uncertainty in INP measurements. In the revision, we used the method proposed by Barker (2002) and O'sullivan et al. (2018) to calculate the confidence intervals.

$$\mu(T) + \frac{(Z_{\alpha/2})^2}{2n} \pm Z_{\alpha/2}\left[4\mu + \frac{(Z_{\alpha/2})^2}{n}\right]^{0.5} / 4n^{0.5}$$

where μ(T) is the number of INPs per droplet, n is the droplet number (90 in our experiments), Zα/2 is the standard score at a confidence level α/2 (1.96 for a 95% confidence interval).

In addition to nucleation stochasticity, other potential sources of uncertainty have been suggested, including aerosol collection and nucleus multiplication. However, these uncertainties are considered negligible, as noted by Vali (1974) and Wright et al. (2014). Furthermore, the influence of dissolved solutes and chemical aging on INP concentrations in rainwater are estimated to be less than an order of magnitude at certain temperatures (Petters and Wright, 2015). Based on these considerations, we did not apply further corrections in this study.

The assumption of a cloud water content (CWC) of 0.4 g m^{-3} has been widely adopted in

numerous studies (e.g., Chen et al., 2021; Chen et al., 2024; Niu et al., 2024; Vepuri et al., 2021; Petters and Wright, 2015). We acknowledge that uncertainties may arise from this assumption, particularly due to its potential seasonal variability. To address this, we have incorporated a discussion of these uncertainties in the revised manuscript.

Precipitation samples were collected using a polyethylene bucket (50 cm in diameter) equipped with a pre-cleaned polyethylene bag, placed at a height of 1.5 m above the ground. During dry periods without precipitation, the bucket was stored indoors with a lid to prevent contamination. At the onset of precipitation, a new clean polyethylene bag was immediately mounted on the bucket, and the sampling time was recorded. Once precipitation ceased, the polyethylene bag containing the sample was promptly retrieved to minimize contamination from dry deposition. Samples were then transferred to pre-sterilized polycarbonate bottles and stored at -20°C until further analysis (Liu et al., 2023). During sampling, the total precipitation amount was measured directly with a rain gauge, and only precipitation events with amounts greater than 1.0 mm were analyzed in this study. Two field blanks were prepared by pouring 100 ml Milli-Q water into a clean polyethylene bag, and the measured concentrations were subtracted from those of the precipitation samples at each freezing temperature (Figure R1 and revised Figure S3; Figure R2 and revised Figure 1). Precipitation samples were not diluted during analysis, thereby avoiding additional sources of error.

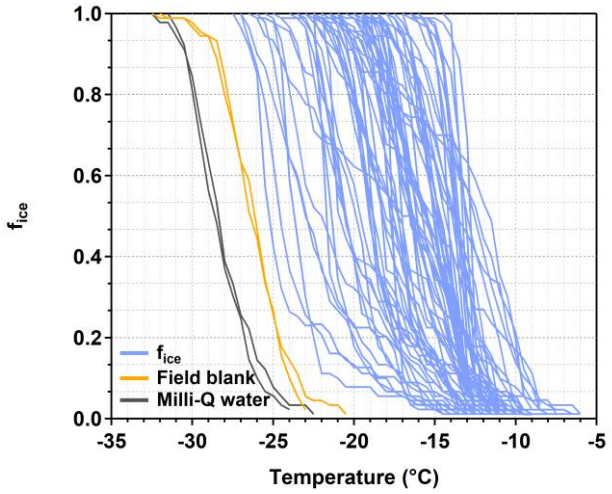

Figure R1. Frozen fractions of rainwater samples (f_{ice}), Milli-Q water and filed blanks as a function of temperature.

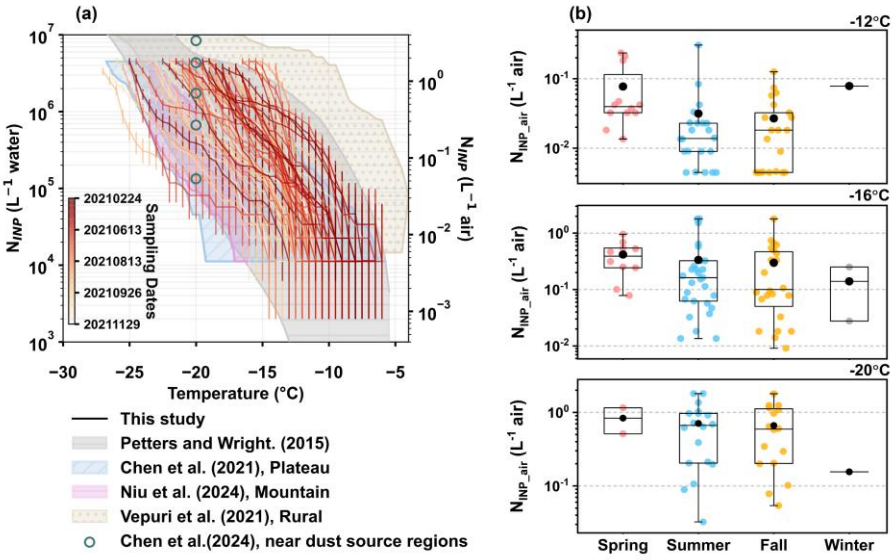

Figure R2. (a) The INPs concentration spectra per volume of air (N_{INP_air}, left axis) and the spectra per volume of water (N_{INP_water}, right axis) as functions of temperature, with the varying colors of the lines correspond to distinct sampling dates. The error bars represent the confidence interval of 95%. The results from this study are compared with N_{INP} spectra from global precipitation samples (dark-gray enclosed area (Petters and Wright, 2015)), precipitation samples in an rural site in Texas, USA (light brown shaded area (Vepuri et al., 2021)), precipitation samples in the Plateau region in the Tibetan Plateau in China (light blue shaded area (Chen et al., 2021)), precipitation samples in a mountain site in the Mt. Lu, China (light purple shaded area (Niu et al., 2024)), and snowpack samples in near-desert dust region over the Tibetan Plateau (cyan hollow circles (Chen et al., 2024)). (b) Box plots of N_{INP_air} at -12 ℃, -16 ℃, and -20 ℃ for different seasons. In each plot, the black line and circle represent the median and mean values, respectively, the bottom and top edges of the box represent the 25th and 75th percentiles, and the upper and lower limits represent the minimum and maximum value.

The following description has been added to the revised manuscript.

Section 2.2:

The GIGINA instrument was calibrated using undecane, dodecane, and tridecane at a heating rate of 1℃/min. Calibration indicated that the actual droplet temperature was 0.2℃ higher than the cold stage set temperature (Chen et al., 2023). Subsequent experimental data were corrected accordingly. Confidence intervals for INP concentrations, accounting for nucleation stochasticity as the primary source of measurement uncertainty, were calculated following the approach of Barker (2002) and O'sullivan et al. (2018).

$$\mu(T) + \frac{(Z_{\alpha/2})^2}{2n} \pm Z_{\alpha/2}\left[4\mu + \frac{(Z_{\alpha/2})^2}{n}\right]^{0.5} /4n^{0.5}$$

where μ(T) is the number of INPs per droplet, n is the droplet number (90 in our experiments), Zα/2 is the standard score at a confidence level α/2 (1.96 for a 95% confidence interval).

The INP per volume of water can be converted to INP per volume of air (N_{INP_air}) using the Eq. (3):

$$N_{INP\_air} = N_{INP\_water} \times F_{cloud-air} \quad (3)$$

The cloud water content (CWC) was assumed to be 0.4 g m^{-3}, a value widely adopted in previous studies (e.g., Chen et al., 2021; Chen et al., 2024; Niu et al., 2024; Vepuri et al., 2021; Petters and Wright, 2015). For cloud droplets with a volume of 1 pL dispersed in 1 m^3 of air, the corresponding cloud water volume per unit air volume ($F_{cloud\text{-}air}$) is 4×10^{-7} m^3 water/m^3 air. Seasonal variability in CWC was not considered in this study.

Section 2.1:

A polyethylene bucket (50 cm in diameter) equipped with a pre-cleaned polyethylene bag was positioned 1.5 m above ground level for sample collection. During dry periods without precipitation, the bucket was stored indoors with a lid to prevent contamination. At the onset of precipitation, a new clean polyethylene bag was immediately mounted on the bucket, and the sampling time was recorded. Once precipitation ceased, the polyethylene bag containing the sample was promptly retrieved to minimize contamination from dry deposition. Samples were then transferred to pre-sterilized polycarbonate bottles and stored at −20 ℃ until further analysis (Liu et al., 2023). During sampling, the total precipitation amount was measured directly with a rain gauge, and only precipitation events with amounts greater than 1.0 mm were analyzed in this study. A total of 67 precipitation samples were collected across four seasons: 11 in spring, 29 in summer, 25 in autumn, and 2 in winter. Two field blanks were prepared by pouring 100 ml Milli-Q water into a clean polyethylene bag, and the measured concentrations were subtracted from those of the precipitation samples at each freezing temperature (Fig. S3). All precipitation samples analyzed in this study were rainfall. The two winter samples are reported only in terms of their concentrations and were excluded from further analysis.

Figure 3 and lines 249-258: The source profiles of many of your PMF factors are so similar that the identities of the different sources are extremely unclear. "mineral dust", "soil dust", "industrial emissions", and "industrial emissions + biomass burning" are all very similar, and the differences between them are not significant enough to identify them with any confidence. The main quantities that could be used to identify many of these factors have not been measured, such as total organic content to distinguish "mineral dust" and "soil dust", or levoglucosan to identify "biomass burning".

Response: We thank the reviewer for the valuable comments. In revision, we removed the two winter samples and re-conducted the PMF analysis. The source profile is shown in Figure R3, and detailed explanation of the basis for factor identification is shown below.

Two types of dust were identified in the PMF results. Factor 1 showed high loadings of mineral elements such as Al, Fe, Mn, Ti, Mg^{2+} and Ca^{2+}, and was identified as mineral dust (Yuan et al., 2008; Huang et al., 2014). Factor 2 was characterized by exhibited elevated levels of water-soluble Mg^{2+} and Ca^{2+}, but lower concentrations of Al, Mn and Fe. In addition, several pollution-related elements, including Zn, Pb, Ni, Cu, and Cl^-, exhibited moderately high loadings. These features suggest that Factor 2 represents road dust, primarily originating from the re-suspended dust and surface soil from unpaved roads (Hien et al., 2001; Yuan et al., 2008). The 24-hour backward trajectories further indicated that air masses dominated by Factor 1 mainly originated from long-range transport from the northwest, whereas those dominated by Factor 2 were dispersed across various directions over short distances, implying a more local origin compared with Factor 1 (Figure R4). This evidence supports the interpretation that Factor

1 corresponds to long-range transported mineral dust, while Factor 2 reflects locally generated road dust.

Factor 3 was dominated by secondary inorganic components (SO_4^{2-}, NO_3^-, and NH_4^+), indicative of secondary source (Salvador et al., 2004). Factor 4 exhibited high loadings of Pb, Cu, Mn, and Co, and was identified as industrial emissions (Zhou and Wang, 2019; Li et al., 2025). These elements were commonly associated with metal smelting and fuel combustion processes (Yuan et al., 2008; Pacyna, 1998; Song et al., 2001). Factor 5 showed elevated levels of Cd, As, V, Cr Zn, Ba, as well as K^+. Cd is typically emitted from high-temperature coal and oil combustion as well as municipal waste incineration (Uberol and Shadman, 1991; Kim et al., 2018). As is widely recognized as a tracer of coal combustion (Harrison et al., 1996). K^+ is often related to biomass burning (Pant and Harrison, 2012), but may also occur as K_2O in coal fly ash (Yu et al., 2019). Thus, these features indicate that Factor 5 represents coal combustion. Factor 6 was characterized by enriched in Na^+ and Cl^- and was identified as sea salt (Waked et al., 2014).

Please note that we have revised the source descriptions as follows: Factor 2 "soil dust" has been reclassified to "road dust", Factor 5 "industrial emissions + biomass burning" has been redefined as "coal combustion".

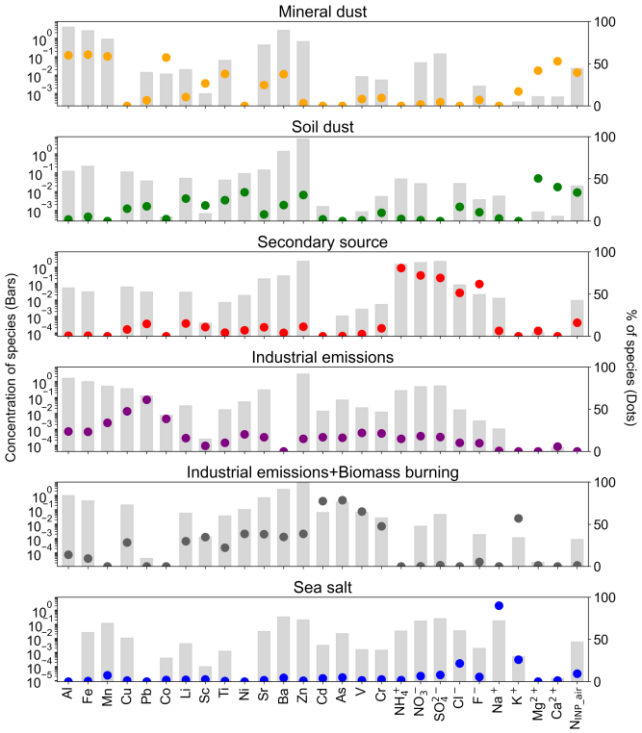

Figure R3. Source profile of positive matrix factorization (PMF) model. Bars represent the concentration of individual species, and dots indicate their percentage contributions. The units are μg/ml for inorganic ions and ng/ml for metal elements.

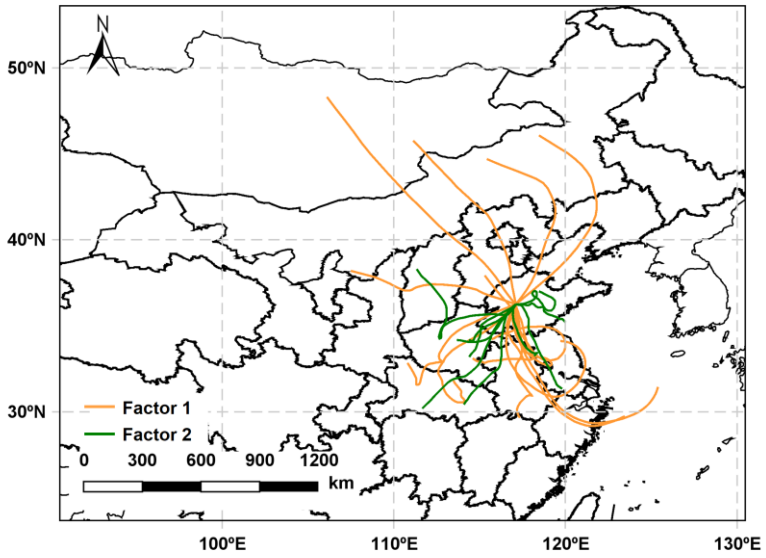

Figure R4. 24-hour backward trajectories of air mass associated with Factor 1 and Factor 2.

In the revised manuscript, the source identification has been revised as follows:

Factor 1 was characterized by high concentrations of mineral elements such as Al, Fe, Mn, Ti, Mg^{2+}, and Ca^{2+}, and was identified as mineral dust (Yuan et al., 2008; Huang et al., 2014). Factor 2 exhibited elevated levels of water-soluble Mg^{2+} and Ca^{2+}, but lower concentrations of Al, Mn and Fe. In addition, several pollution-related elements, including Zn, Pb, Ni, Cu, and Cl-, exhibited moderately high loadings. These features suggest that Factor 2 represents road dust, primarily originating from the re-suspended dust and surface soil from unpaved roads (Yuan et al., 2008; Hien et al., 2001). The 24-hour backward trajectories further indicated that air masses dominated by Factor 1 were primarily associated with long-range transport, whereas those dominated by Factor 2 originated from more local sources (Figure S11). Factor 3 was dominated by secondary inorganic components (SO_4^{2-}, NO_3^-, and NH_4^+), indicative of secondary aerosols (Salvador et al., 2004). Factor 4 showed high levels of Pb, Cu, Mn, and Co, and was identified as industrial emissions (Zhou and Wang, 2019; Li et al., 2025). These elements were commonly associated with metal smelting and fuel combustion processes (Yuan et al., 2008; Pacyna, 1998; Song et al., 2001). Factor 5 exhibited elevated levels of Cd, As, V, Cr, Zn, Ba, as well as K^+. Cd is typically emitted from high-temperature coal and oil combustion as well as municipal waste incineration (Uberol and Shadman, 1991; Kim et al., 2018). As is widely recognized as a tracer of coal combustion (Harrison et al., 1996). K^+ is often related to biomass burning (Pant and Harrison, 2012), but may also occur as K_2O in coal fly ash (Yu et al., 2019). Thus, these features indicate that Factor 5 represents coal combustion. Factor 6 was characterized by enriched in Na^+ and Cl^- and was identified as sea salt (Waked et al., 2014).

Beyond these critical and related issues, there is a larger problem applying PMF analysis to INP concentrations. INP do not necessarily correlate with any of the major components measured. If this is the case, PMF analysis will distribute INP randomly across sources, and the interpretation of INP within the source profiles will be meaningless. Rigorous error analysis of PMF assignment uncertainties would be required to show that any interpretation of INP

results within PMF analysis is meaningful.

Response: We thank the reviewer for the valuable comments. To evaluate the applicability and robustness of this approach, we conducted two additional checks:

(1) We removed the two winter samples and re-conducted the PMF source apportionment analysis using the sampling data both with and without the inclusion of the N_{INP_air} parameter. The resulting source profiles are shown in Figure R5a-b. The two profiles were essentially identical, and each factor was determined consistently with our previous response. These results indicate that N_{INP_air} has minimal impact on the classification of PMF factors.

(2) In the PMF analysis including N_{INP_air} concentration, 95% of the residuals for all parameters fell within the range of -3 to +3. Specifically, the residuals of N_{INP_air} ranged from -2.3 to +2.7, which lies well within the acceptable range of -3 to 3 suggested by Zhang et al. (2024b). These results support the conclusion that the interpretation of INP data within the PMF framework is robust and meaningful.

In addition, in response to the reviewer's further comments, we performed a correlation analysis between the daily contribution percentage of the Factor 1 (mineral dust) and the N_{INP_air} concentration at various freezing temperatures. As shown in Figure R5c, positive correlations were observed across all freezing temperatures, with statistically significant correlations in the range of –11 °C to –19.5 °C. These results further demonstrate that mineral dust plays an important role in contributing to INPs in our study region. The new analyses have been incorporated into the revised manuscript (see revised Figure 3, Figure S3, and the main text).

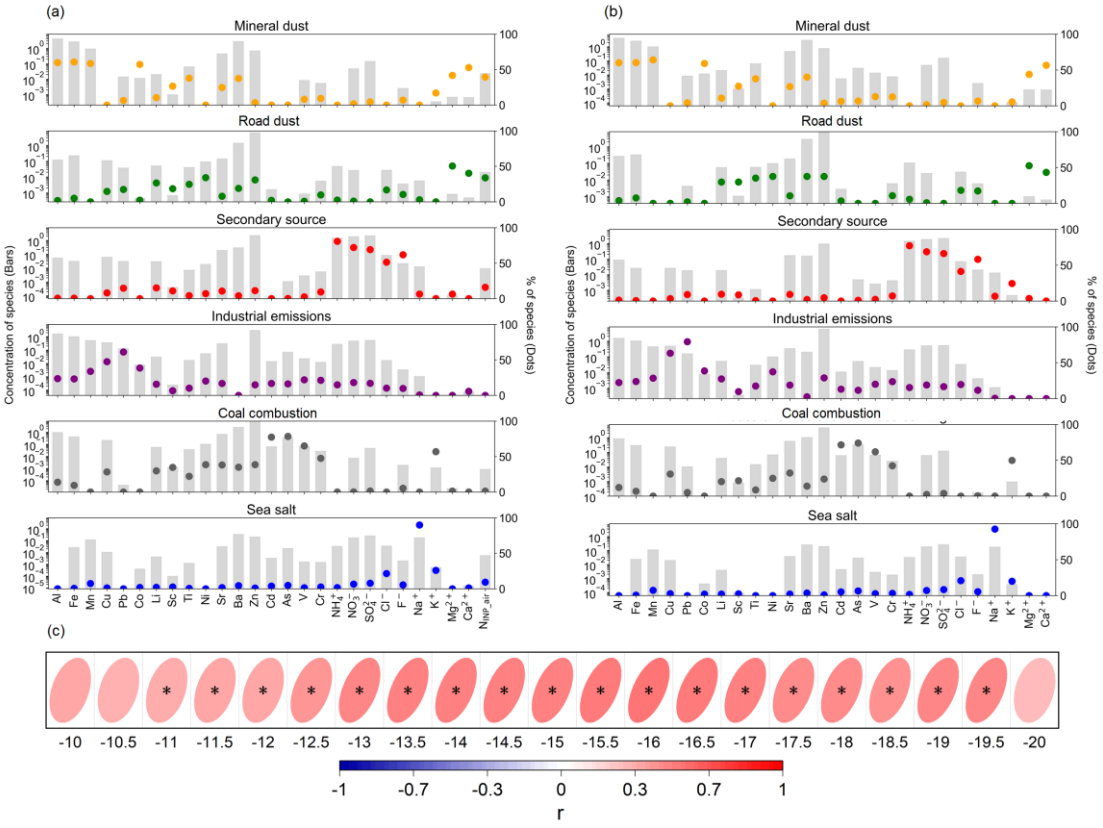

Figure R5. Source apportionment of 17 metallic elements and 9 water-soluble ions, with and

without $N_{INP\text{-}air}$ (-16 °C) using the positive matrix factorization (PMF) model. (a, b) Source profiles of the six factors. Bars represent the concentration of individual species, and dots indicate their percentage contributions. The units are μg/ml for inorganic ions and ng/ml for metal elements. (c) Correlation between daily contribution percentage of Factor 1 (mineral dust) and N_{INP_air} concentration at different freezing temperatures.

Revised manuscript:

The PMF model was applied to quantify the contributions of major sources to the measured N_{INP_air}. Six sources were identified, with their profiles respectively illustrated in Figure 3a. The source profile is basically the same with Figure S10, in which PMF model was conducted without N_{INP_air}, indicating the negligible impact on the classification of PMF factors.

Factor 1 was characterized by high concentrations of mineral elements such as Al, Fe, Mn, Ti, Mg^{2+}, and Ca^{2+}, and was identified as mineral dust (Yuan et al., 2008; Huang et al., 2014). Factor 2 exhibited elevated levels of water-soluble Mg^{2+} and Ca^{2+}, but lower concentrations of Al, Mn and Fe. In addition, several pollution-related elements, including Zn, Pb, Ni, Cu, and Cl-, exhibited moderately high loadings. These features suggest that Factor 2 represents road dust, primarily originating from the re-suspended dust and surface soil from unpaved roads (Hien et al., 2001; Yuan et al., 2008). Factor 3 was dominated by secondary inorganic components (SO_4^{2-}, NO_3^-, and NH_4^+), indicative of secondary aerosols (Salvador et al., 2004). Factor 4 showed high levels of Pb, Cu, Mn, and Co, and was identified as industrial emissions (Zhou and Wang, 2019; Li et al., 2025). These elements were commonly associated with metal smelting and fuel combustion processes (Pacyna, 1998; Song et al., 2001; Yuan et al., 2008). Factor 5 exhibited elevated levels of Cd, As, V, Cr, Zn, Ba, as well as K^+. Cd is typically emitted from high-temperature coal and oil combustion as well as municipal waste incineration (Uberol and Shadman, 1991; Kim et al., 2018). As is widely recognized as a tracer of coal combustion (Harrison et al., 1996). K^+ is often related to biomass burning (Pant and Harrison, 2012), but may also occur as K_2O in coal fly ash (Yu et al., 2019). Thus, these features indicate that Factor 5 represents coal combustion. Factor 6 was characterized by enriched in Na^+ and Cl^- and was identified as sea salt (Waked et al., 2014).

Figure 3c illustrates the contributions of the six sources to N_{INP_air}. At a freezing temperature of −16 °C, mineral dust was the dominant contributor, accounting for 43.6% of N_{INP_air}. This contribution increased markedly to 71.7% in spring, underscoring the dominant role of mineral dust (Figure S12b). To further examine this relationship, we performed a correlation analysis between the daily contribution percentage of the mineral dust factor obtained from PMF modeling and N_{INP_air} at different freezing temperatures (Figure 3d). The significant positive correlations observed within -11 °C to -19.5 °C further indicate that mineral dust is a major contributor to INPs.

Minor comments:

Line 45: Hoose 2010 reference is wildly mis-characterized, this statement needs to be reworked or removed. Something akin to "Simulations performed by Hoose et al., 2010, found that model outputs were broadly consistent with experimental measurements of INP concentrations when initialized with 77% mineral INP composition." would be acceptable.

Response: Thanks. We have revised it as follows:

Simulations by Hoose et al. (2010) showed that on global average 77% of the heterogeneous nucleation is initiated by mineral dust particles, which are broadly consistent with experimental measurements.

Lines 62-65: the assertation that background dust is overlooked as an INP source is easily refuted by many of your other citations in the introduction…

Response: Thanks. We have removed this statement from the revised manuscript.

Line 67-68: many anthropogenic aerosols are very poor INPs, this unsupported claim should probably be removed.

Response: Thanks. We have removed "anthropogenic" from this statement.

Section 2.1: give sampling site coordinates and elevation.

Response: Thanks, we added the sampling site coordinates and elevation in the revised manuscript.

In this study, precipitation samples were collected at the summit of Mount Tai (36.25°N, 117.10°E, 1534 m a.s.l.) from February 24 to November 29 in 2021.

Line 97-98: referencing WBF is odd here… glass slide is probably more important for preventing evaporation/condensation with room air. I recommend reworking.

Response: We have revised the statement as follows:

The spacer was then sealed with another glass slide to minimize droplet evaporation and to prevent ice seeding from neighboring droplets (Gong et al., 2020).

Line 116: should be either "using ion chromatography" or using an ion chromatograph"

Response: Thanks, we have revised it to "using ion chromatography".

Line 141-142: justification of this treatment of missing data should be provided.

Response: Thank you for your comment. The missing data were excluded from the PMF analysis, and we have removed the corresponding statement from the manuscript.

Line 143: "Q ratio" needs to be discussed prior to this in order for it to make sense. Also do you mean "As the number of PMF factors increase" instead of "As the PMF factor increases?"

Response: Yes, we have added the discuss about "Q ratio" in the revised manuscript. We revised the statement as "As the number of PMF factors increase" in the revised manuscript.

We have revised the manuscript as follows:

The PMF solution minimizes the objective function Q via a conjugate gradient algorithm, based upon the estimated data uncertainties (or adjusted data uncertainties), as displayed in Eq. (7):

$$Q = \sum_{i=1}^{n} \sum_{j=1}^{m} \left(\frac{X_{ij} - \sum_{k=1}^{p} g_{ik} f_{kj}}{U_{ij}} \right)^2 \quad (7)$$

where X_{ij} is the measured concentration values, U_{ij} is the estimated uncertainty values, g_{ik} is the factor score (source contribution) values, f_{kj} is the factor loading (source profile) values, and n, m, and p denote the numbers of samples, species, and sources, respectively. Q/Q_{exp} is a standardized metric used to evaluate the goodness of fitness in PMF models, representing the ratio of the objective function Q to the theoretical value Q_{exp} under ideal fitting conditions, and can be computed by the model. Q ratio denotes the rate of change in Q/Q_{exp} from the previous factor to the current factor. In this study, solutions involving 3-10 sources were tested. As the number of PMF factors increases, the Q ratio stabilizes when the PMF factor reaches 6, as illustrated in Figure S2, indicating enhanced stability in the fundamental operation. Therefore, 6 factors were proposed as the optimal solution in this study.

Line 216: HR and HS aren't defined acronyms, so while I understand which quantities they refer to it makes further discussion using these terms difficult to follow.

Response: Thank you for your comment. We have added the full forms of HR-N_{INP_air} (heat-resistant INPs) and HS-N_{INP_air} (heat-sensitive INPs) to enhance the readability in the revised manuscript.

Revised manuscript:

This approach allows for the identification of heat-sensitive INPs (HS-N_{INP_air}), which primarily refer to proteinaceous biological materials such as lichens and bacteria, and heat-resistant INPs (HR-N_{INP_air}) from other sources, including polysaccharides, macromolecular organic particles, mineral dust, sea spray aerosols, and volcanic ash. The remaining INPs concentrations after heat treatment are referred to as heat-resistant INPs, and the difference between total N_{INP_air} and HR-N_{INP_air} represents HS-N_{INP_air}.

Figure 1.b) you only have two winter samples, the data isn't really meaningful, I would recommend removing it.

Response: Thanks. We agree and have removed the winter samples from the analysis in the revised manuscript. We have added the following statement in revision.

The two winter samples are reported only in terms of their concentrations and were excluded from further analysis.

Figure 2.b): is this calculated as mean(HR/HS) or as mean(HR)/mean(HS)? They would have different interpretations so clarification is required. Additionally, the uncertainties with these ratios will be very large and cannot be ignored.

Response: Thanks. Figure 2b is calculated as mean of daily HR/HS values. We have added the standard deviations at each freezing temperature. The revised figure is shown below.

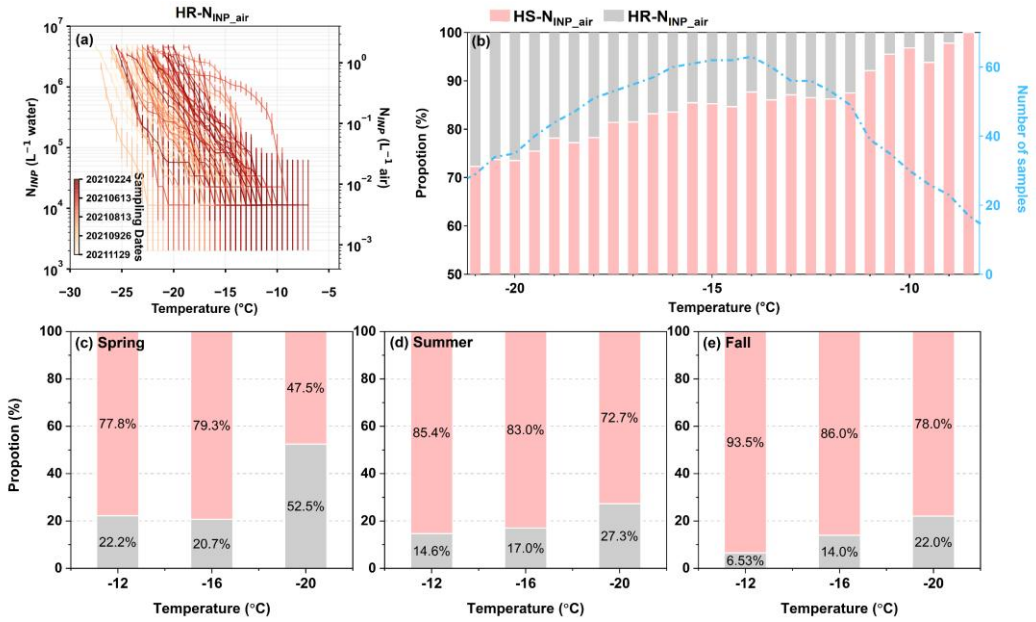

Figure R6. (a) Heat-resistant INPs (HR-N_{INP_air}) derived using the wet-heat method as functions of temperature, with the varying colors of the lines correspond to distinct sampling dates. The error bars represent the confidence interval of 95%. (b) Proportion of heat-sensitive INPs (HS-N_{INP_air}) and HR-N_{INP_air} as functions of temperature, and number of samples when calculating the proportions. (c-e) Seasonal proportions of HS-N_{INP_air} and HR-N_{INP_air} at -12 ℃, -16 ℃, and -20 ℃.

Figure 3: Y axis on these figures has no units.

Response: We have added the units in the figure captions. The units are μg/ml for inorganic ions and ng/ml for metallic elements.

Reference:

Barker, L.: A Comparison of Nine Confidence Intervals for a Poisson Parameter When the Expected Number of Events is ⩽ 5, The American Statistician, 56, 85-89, 10.1198/000313002317572736, 2002.

Chen, J., Wu, Z. J., Wu, G. M., Gong, X. D., Wang, F., Chen, J. C., Shi, G. L., Hu, M., and Cong, Z. Y.: Ice-Nucleating Particle Concentrations and Sources in Rainwater Over the Third Pole, Tibetan Plateau, J Geophys Res-Atmos, 126, 13, https://doi.org/10.1029/2020jd033864, 2021.

Chen, J., Xu, J., Wu, Z., Meng, X., Yu, Y., Ginoux, P., DeMott, P. J., Xu, R., Zhai, L., Yan, Y., Zhao, C., Li, S.-M., Zhu, T., and Hu, M.: Decreased dust particles amplify the cloud cooling effect by regulating cloud ice formation over the Tibetan Plateau, Sci Adv, 10, eado0885, https://doi.org/10.1126/sciadv.ado0885, 2024.

Chen, L., Peng, C., Chen, J., Chen, J., Gu, W., Jia, X., Wu, Z., Wang, Q., and Tang, M.: Effects of heterogeneous reaction with NO2 on ice nucleation activities of feldspar and Arizona Test Dust, J Environ Sci-China, 127, 210-221, https://doi.org/10.1016/j.jes.2022.04.034, 2023.

Gong, X., Wex, H., van Pinxteren, M., Triesch, N., Fomba, K. W., Lubitz, J., Stolle, C., Robinson, T. B., Müller, T., Herrmann, H., and Stratmann, F.: Characterization of aerosol particles at Cabo Verde close to sea level and at the cloud level – Part 2: Ice-nucleating particles in air, cloud and seawater, Atmos. Chem. Phys., 20, 1451-1468, 10.5194/acp-20-1451-2020, 2020.

Harrison, R. M., Smith, D. J. T., and Luhana, L.: Source apportionment of atmospheric polycyclic

aromatic hydrocarbons collected from an urban location in Birmingham, UK, Environ Sci Technol, 30, 825-832, 10.1021/es950252d, 1996.

Hien, P. D., Binh, N. T., Truong, Y., Ngo, N. T., and Sieu, L. N.: Comparative receptor modelling study of TSP, PM2 and PM2−10 in Ho Chi Minh City, Atmospheric Environment, 35, 2669-2678, https://doi.org/10.1016/S1352-2310(00)00574-4, 2001.

Huang, R.-J., Zhang, Y., Bozzetti, C., Ho, K.-F., Cao, J.-J., Han, Y., Daellenbach, K. R., Slowik, J. G., Platt, S. M., Canonaco, F., Zotter, P., Wolf, R., Pieber, S. M., Bruns, E. A., Crippa, M., Ciarelli, G., Piazzalunga, A., Schwikowski, M., Abbaszade, G., Schnelle-Kreis, J., Zimmermann, R., An, Z., Szidat, S., Baltensperger, U., Haddad, I. E., and Prévôt, A. S. H.: High secondary aerosol contribution to particulate pollution during haze events in China, Nature, 514, 218-222, 10.1038/nature13774, 2014.

Kim, S., Kim, T. Y., Yi, S. M., and Heo, J.: Source apportionment of PM2.5 using positive matrix factorization (PMF) at a rural site in Korea, J Environ Manage, 214, 325-334, 10.1016/j.jenvman.2018.03.027, 2018.

Li, Y., Wang, Z., Liu, L., Geng, Y., and Zhang, J.: A combined model method was used to identify the main influencing factors of soil heavy metal pollution sources in Qian river, China, Sci Rep, 15, 14040, https://doi.org/10.1038/s41598-025-98881-5, 2025.

Niu, M., Hu, W., Huang, S., Chen, J., Zhong, S., Huang, Z., Duan, P., Pei, X., Duan, J., Bi, K., Chen, S., Jin, R., Sheng, M., Yang, N., Wu, L., Deng, J., Zhu, J., Shen, F., Wu, Z., Zhang, D., and Fu, P.: Deciphering the Significant Role of Biological Ice Nucleators in Precipitation at the Organic Molecular Level, 129, e2024JD041278, https://doi.org/10.1029/2024JD041278, 2024.

O'Sullivan, D., Adams, M. P., Tarn, M. D., Harrison, A. D., Vergara-Temprado, J., Porter, G. C. E., Holden, M. A., Sanchez-Marroquin, A., Carotenuto, F., Whale, T. F., McQuaid, J. B., Walshaw, R., Hedges, D. H. P., Burke, I. T., Cui, Z., and Murray, B. J.: Contributions of biogenic material to the atmospheric ice-nucleating particle population in North Western Europe, Sci Rep, 8, 13821, 10.1038/s41598-018-31981-7, 2018.

Pacyna, J. M., Harrison, R. M. v. G., R. E. (Ed.): Source inventories for atmospheric trace metals, IUPAC Series on Analytical and Physical Chemistry of Environmental Systems, Wiley, Chichester, UK1998.

Pant, P. and Harrison, R. M.: Critical review of receptor modelling for particulate matter: A case study of India, Atmospheric Environment, 49, 1-12, 10.1016/j.atmosenv.2011.11.060, 2012.

Petters, M. D. and Wright, T. P.: Revisiting ice nucleation from precipitation samples, Geophys Res Lett, 42, 8758-8766, https://doi.org/10.1002/2015GL065733, 2015.

Salvador, P., Artíñano, B., Alonso, D. G., Querol, X., and Alastuey, A.: Identification and characterisation of sources of PM10 in Madrid (Spain) by statistical methods, Atmospheric Environment, 38, 435-447, 10.1016/j.atmosenv.2003.09.070, 2004.

Song, X.-H., Polissar, A. V., and Hopke, P. K.: Sources of fine particle composition in the northeastern US, Atmospheric Environment, 35, 5277-5286, https://doi.org/10.1016/S1352-2310(01)00338-7, 2001.

Uberol, M. and Shadman, F.: HIGH-TEMPERATURE REMOVAL OF CADMIUM COMPOUNDS USING SOLID SORBENTS, Environ Sci Technol, 25, 1285-1289, 10.1021/es00019a009, 1991.

Vali, G.: Comments on "Freezing Nuclei Derived from Soil Particles" %J Journal of Atmospheric Sciences, 31, 1457-1459, https://doi.org/10.1175/1520-0469(1974)031<1457:CONDFS>2.0.CO;2, 1974.

Vepuri, H. S. K., Rodriguez, C. A., Georgakopoulos, D. G., Hume, D., Webb, J., Mayer, G. D., and

Hiranuma, N.: Ice-nucleating particles in precipitation samples from the Texas Panhandle, Atmos. Chem. Phys., 21, 4503-4520, https://doi.org/10.5194/acp-21-4503-2021, 2021.

Waked, A., Favez, O., Alleman, L. Y., Piot, C., Petit, J. E., Delaunay, T., Verlinden, E., Golly, B., Besombes, J. L., Jaffrezo, J. L., and Leoz-Garziandia, E.: Source apportionment of PM₁₀ in a north-western Europe regional urban background site (Lens, France) using positive matrix factorization and including primary biogenic emissions, Atmos. Chem. Phys., 14, 3325-3346, 10.5194/acp-14-3325-2014, 2014.

Wright, T. P., Hader, J. D., McMeeking, G. R., and Petters, M. D.: High Relative Humidity as a Trigger for Widespread Release of Ice Nuclei, Aerosol Sci. Technol., 48, i-v, 10.1080/02786826.2014.968244, 2014.

Yu, Y. Y., He, S. Y., Wu, X. L., Zhang, C., Yao, Y., Liao, H., Wang, Q. G., and Xie, M. J.: PM2.5 elements at an urban site in Yangtze River Delta, China: High time-resolved measurement and the application in source apportionment, Environ. Pollut., 253, 1089-1099, 10.1016/j.envpol.2019.07.096, 2019.

Yuan, H., Zhuang, G., Li, J., Wang, Z., and Li, J.: Mixing of mineral with pollution aerosols in dust season in Beijing: Revealed by source apportionment study, Atmospheric Environment, 42, 2141-2157, https://doi.org/10.1016/j.atmosenv.2007.11.048, 2008.

Zhang, J., Zong, Z., Pei, C., Li, Q., Huang, L., Mu, J., Sun, Y., Liu, Y., Chen, H., Lu, D., Xue, L., and Wang, W.: Sources and formation characteristics of particulate nitrate in the Pearl River Delta region of China: Insights from three-year online observations, Sci Total Environ, 945, 174107, https://doi.org/10.1016/j.scitotenv.2024.174107, 2024a.

Zhang, X., Gao, H., Qi, A., Duan, S., Zhang, W., Zhang, Y., Huang, Q., Zhao, T., Han, G., Wang, W., and Yang, L.: Origins and health risk assessment of PAHs/APAHs/NPAHs/OPAHs in PM2.5 at a background site in North China Plain: Implications for crude oil emissions, Atmos. Pollut. Res., 15, 102081, https://doi.org/10.1016/j.apr.2024.102081, 2024b.

Zhou, X.-Y. and Wang, X.-R.: Impact of industrial activities on heavy metal contamination in soils in three major urban agglomerations of China, Journal of Cleaner Production, 230, 1-10, https://doi.org/10.1016/j.jclepro.2019.05.098, 2019.